Density of oxidation-induced stacking faults in damaged silicon

Kuper, F. G.; de Hosson, J. Th. M. ; Verwey, J. F.

Published in:
Journal of Applied Physics

DOI:
10.1063/1.337284

Publication date:
1986

Citation for published version (APA):
Kuper, F. G., de Hosson, J. T. M., & Verwey, J. F. (1986). Density of oxidation-induced stacking faults in damaged silicon. Journal of Applied Physics, 60(4), 1530-1532. https://doi.org/10.1063/1.337284

Density of oxidation-induced stacking faults in damaged silicon

F. G. Kuper, J. Th. M. De Hosson, and J. F. Verwey

Citation: Journal of Applied Physics **60**, 1530 (1986); doi: 10.1063/1.337284
View online: https://doi.org/10.1063/1.337284
View Table of Contents: http://aip.scitation.org/toc/jap/60/4
Published by the American Institute of Physics

these expressions for $\overline{N}_k$ and γ_k, and integrating Eq. (5) over a pulse duration τ_p one gets

$$N_k(\tau_p) \sim v_d^2 \frac{\exp[\gamma(v_d - v_s)\tau_p] - 1}{\gamma(v_d - v_s)}. \qquad (6)$$

For weak temperature gradient, such that $v_d < v_s$, the argument of the exponential is negative (i.e., one has damping) so that N_k varies as v_d^2 and therefore as J_p^2. On the other hand, for high enough values of the temperature gradient, such that $v_d > v_s$, the argument of the exponential may become positive (i.e., amplification) with the result that N_k grows exponentially with v_d ($\sim J_p$). These features, together with the reasonable agreement between the calculated and the experimentally observed values of the threshold condition $v_d > v_s$, are, in our opinion, strong evidence in support of our claim for interpreting the present results as due to the thermoelectric amplification of acoustic waves.

[1]A. R. Hutson, J. H. McFee, and D. L. White, Phys. Rev. Lett. **7**, 237 (1961).

[2]H. N. Spector, in *Solid State Physics*, edited by F. Seitz and F. Turnbull (Academic, New York, 1966), Vol. 19, p. 291.

[3]V. L. Bonch-Bruevich and Yu. V. Gulyaev, Radiotekh. Elektron. **8**, 1179 (1963).

[4]S. Sharma and S. P. Singh, J. Appl. Phys. **45**, 4656 (1974).

[5]E. M. Ephstein, Sov. Phys. Semicond. **9**, 1043 (1976).

[6]M. A. Tenan, A. Marotta, and L. C. M. Miranda, Appl. Phys. Lett. **35**, 321 (1979).

[7]M. Born and E. Wolf, *Principles of Optics* (Pergamon, Oxford, 1975), p. 614.

Density of oxidation-induced stacking faults in damaged silicon

F. G. Kuper, J. Th. M. De Hosson, and J. F. Verwey
Department of Applied Physics, Materials Science Centre, University of Groningen, Nijenborgh 18, 9747 AG Groningen, The Netherlands

(Received 21 March 1986; accepted for publication 6 May 1986)

A model for the relation between density and length of oxidation-induced stacking faults on damaged silicon surfaces is proposed, based on interactions of stacking faults with dislocations and neighboring stacking faults. The model agrees with experiments.

Thermal oxidation of diamond-lapped silicon wafers leads to the growth of extrinsic stacking faults.[1] Much research has been done on these stacking faults in an exploratory manner, but only recently, in 1984, Ishihara, Kaneko, and Matsumoto[2] discovered that density and length of stacking faults in diamond-lapped wafers are related to each other, independent of oxidation temperature or surface orientation. This paper explains these experimental findings and reports some experimental results obtained by ourselves. Annihilation of extrinsic stacking faults occurs, if we neglect retrogrowth, via a Hirsch reaction:

$$1/3[111] + 1/6[\bar{1}2\bar{1}] + 1/6[\bar{1}\bar{1}2] \rightarrow 1/2[011]. \qquad (1)$$

Two Shockley partial dislocations, one above and one below the (111) stacking fault plane, eliminate the stacking fault, leaving behind a perfect dislocation bounding the former stacking fault. These two Shockley dislocations must be created by an event during the oxidation. One possibility is an impingement of two stacking faults, the other is the impingement of a stacking fault and a perfect dislocation.

Stacking fault–stacking fault interactions can be divided in two categories. We call them obtuse [(111) with $(\bar{1}\bar{1}1)$] and acute [(111) with $(1\bar{1}1)$ or $(\bar{1}11)$]. On oxidized (001) silicon wafers with many stacking faults, many acute impingements can be seen that apparently did not give rise to unfaulting reactions. On the other hand, on (001) planes obtuse interaction always seems to cause annihilation, as demonstrated by Hayafuji and Kawado.[3] In addition, no obtuse collisions on our etched (001) samples were observed.

Next, it is known that stacking fault dislocation interaction can cause unfaulting. Attention should be paid to the fact that not all dislocations react in the same way. Some lead to an incorrect unfaulting of the stacking fault. Tan[4] showed that a Shockley dislocation can turn a stacking fault into a four-layer-thick microtwin, i.e., leading to an incorrect unfaulting. In contrast, the same Shockley dislocation can, after dissociation into two other Shockley dislocations, lead to a correct unfaulting reaction as in reaction (1). Finally, it has to be emphasized that some dislocations do not react at all with stacking faults.

In summary:

(i) An obtuse interaction of stacking faults leads to unfaulting, leaving behind two dislocations.

(ii) An acute interaction of stacking faults does not necessarily lead to unfaulting.

(iii) Only a fraction F of the dislocations will cause unfaulting of a colliding stacking fault.

The experiments of Ishihara, Kaneko, and Matsumoto[2] were done with Czochralski (CZ) silicon. The high concentration of carbon and oxygen in this material favors the stacking fault formation. Dieleman and Martens[5] showed that oxidation of (100) float-zone (FZ) silicon induces no stacking faults if the surface is not damaged. So this material is more appropriate to study effects of damage on stacking faults. Therefore, we polished ⟨100⟩ FZ-silicon wafers, B-doped, 1–30 Ω cm, with 3-μm diamond powder prior to oxidation at various temperatures. To avoid stress anneal, the wafers were brought into the furnace already under (dry)

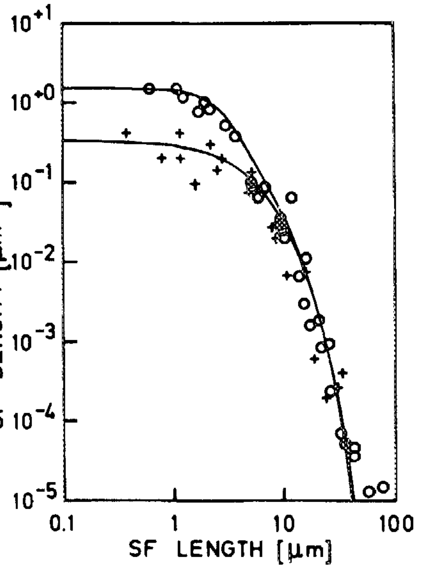

FIG. 1. Experimental data of stacking fault density vs stacking fault length of Ishihara, Kaneko, and Matsumoto (Ref. 2) [Czochralski (100): O] and present work [Float Zone (100): +]. Solid lines represent the theoretical fits.

oxidizing conditions. The results of stacking fault measurements on these samples are depicted in Fig. 1, together with the data of Ishihara, Kaneko, and Matsumoto.[2] On an average we measure 3× lower densities at small lengths, but coincidence at lengths beyond 6 μm.

Based on our observations of the various interactions and assuming that dislocations and stacking faults are uniformly spread over the surface, the following model can be put forward. We define a mean free path λ as the distance a stacking fault can grow until annihilation occurs. The change in stacking fault density dn after stacking fault growth dl can be expressed as

$$dn/n = -dl/\lambda. \tag{2}$$

(i) Obtuse interaction of stacking faults (see Fig. 2). Interaction of a stacking fault can only take place with 25% of all n stacking faults per unit area. Therefore,

$$\lambda^* + l^* = \frac{4}{n} \times \frac{1}{l} \times \frac{1}{2}. \tag{3}$$

Since for stacking faults l^*/l equals about 5, we get for the mean free path for obtuse interaction:

$$\lambda = (10/nl) - l. \tag{4}$$

(ii) Acute interaction of stacking faults with density n and length l has a mean free path:

$$\lambda = (2/n) \times (1/l). \tag{5}$$

However, as we observe so many of these interactions without unfaulting occurring, we will neglect this contribution.

(iii) The mean free path for collision with a dislocation can be evaluated if the total dislocation length T is known:

$$\lambda = 1/T. \tag{6}$$

However, since dislocations tend to be aligned along $\langle 011 \rangle$ and only a fraction F will, after collision, cause unfaulting, the mean free path due to stacking fault dislocation interaction can be written as

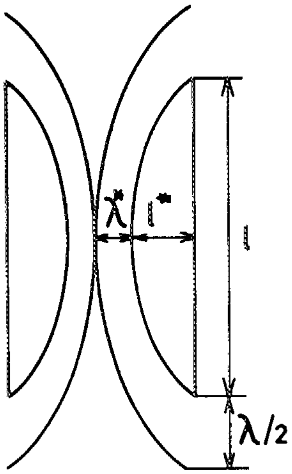

FIG. 2. Obtuse impingement projected on the (001) plane. l is the stacking fault length, l^* is the projected stacking fault width, λ is the mean free path, and λ^* the mean free width of these stacking faults.

$$\lambda = (2/T) \times (1/F). \tag{7}$$

The combination of Eqs. (2), (4), and (7) gives

$$dn/dl = -\tfrac{1}{2} nTF - n^2 l/(10 - nl^2), \tag{8}$$

with the total dislocation length T:

$$T = T_0 + \int_0^l -\frac{dn}{dl}\, l\, dl, \tag{9}$$

where T_0 is the total dislocation length before oxidation.

This differential equation (8) cannot be solved analytically, but it is easily integrated numerically. Only three parameters need to be set: a stacking fault density at $l = 0$, the total dislocation length at $l = 0$ (T_0), and the effective fraction F of the dislocations. It turns out that the data of Ishihara, Kaneko, and Matsumoto can be fitted quite nicely with a starting density of $1.5/\mu\text{m}^2$, an initial dislocation length not beyond a few $\mu\text{m}/\mu\text{m}^2$, and an effective fraction of 10%.

The result of such an integration is depicted also in Fig.

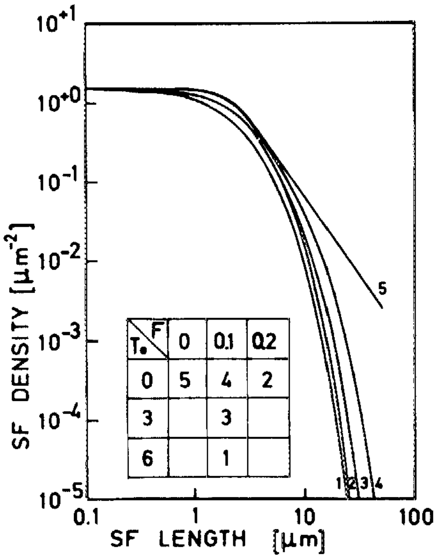

FIG. 3. Calculations of stacking fault density vs stacking fault length with an initial density of $1.5/\mu\text{m}^2$ for various values of F and T_0.

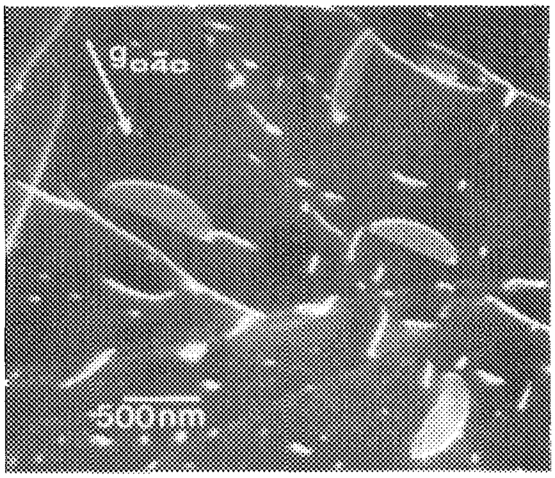

FIG. 4. Transmission electron micrograph of dislocations and stacking faults.

1. The calculated curve is not very sensitive for T_0 but it is for F. The calculated curves for $F = 0$, 10, and 20% are depicted in Fig. 3 ($T_0 = 0$) together with $T_0 = 0$, 3, and 6 μm/μm^2 ($F = 10\%$).

In order to determine T_0 we examined one of our high-density samples in a transmission electron microscope. A dark-field image is depicted in Fig. 1. T_0 was estimated to be 3 μm/μm^2. A calculation with $F = 10\%$ and an initial density of 0.33/μm^2 is also depicted in Fig. 3. We find a good agreement of theory and experiments. Apparently there is only a minor difference between FZ and CZ silicon. The density of the latter tends to be slightly larger after a short oxidation.

Acute interaction has been neglected. In fact, if we compare expressions (4) and (5) we see that both acute and obtuse interaction are of the same character. Further, from Fig. 3 it can be concluded that stacking fault–stacking fault interaction yields only a minor contribution to the rapid decrease of the stacking fault density (viz., $F = 0$ in comparison with $F = 0.1$). Consequently, possible contributions due to acute interactions may be neglected in the calculations.

To unfault a specific stacking fault one needs one out of three possible Shockley dislocations. There are 24 different Shockley dislocations, so as a rough guess we can expect the effective fraction of the dislocations to be 3/24 = 12.5%. As the same Shockley dislocations can cause incorrect unfaulting as well, this 12.5% is an upper limit, in good agreement with our model.

The density of stacking faults as a function of stacking fault length can be described by a model based on stacking fault–dislocation interaction and obtuse stacking fault–stacking fault interaction. It turns out that only an effective fraction of about 10% of the dislocations can cause unfaulting of a particular stacking fault.

We would like to thank L. H. M. Osse for his measurements of density and length of stacking faults. This work is part of the research program of the Foundation for Fundamental Research on Matter (FOM-Utrecht) and has been made possible by financial support from the Netherlands Organization for the Advancement of Pure Research (ZWO-The Hague).

[1] D. J. D. Thomas, Phys. Status Solidi **3**, 2261 (1963).
[2] I. Ishihara, H. Kaneko, and S. Matsumoto, Jpn. J. Appl. Phys. **23**, L620 (1984).
[3] Y. Hayafuji and S. Kawado, J. Appl. Phys. **53**, 1215 (1982).
[4] T. Y. Tan, Appl. Phys. Lett. **34**, 714 (1979).
[5] J. Dieleman and T. H. G. Martens, Appl. Phys. Lett. **40**, 340 (1982).

Application of the electrostatic energy analyzer to cluster size measurement

K. Yano and S. H. Be
The Institute of Physical and Chemical Research, Wako-shi, Saitama 351-01, Japan

(Received 30 December 1985; accepted for publication 21 April 1986)

An electrostatic energy analyzer with a deflection angle of 90° and a resolving power of about 4% up to 200 keV was used to analyze the distribution from a cluster ion source. The experiments were carried out with cluster-ion beams of nitrogen extracted from a specially designed cluster ionizer for controlling the cluster sizes. It is shown that the cluster size as large as $\sim 10^5$ atoms/cluster is measurable with this energy analyzer.

Injection of a high-power energetic cluster beam is now being developed as a method for efficient heating of plasmas and fueling steady-state fusion reactors.[1-3] The cluster beam has a wide mass distribution because individual clusters are produced by the adiabatic expansion of a precooled, high-pressure gas through a nozzle into a low-pressure region. For an application of cluster-ion beams to fusion reactors, cluster ions should be disintegrated into molecules or atoms in the plasma after injection of cluster-ion beams. Because of this, it is important to know a mass distribution of the cluster beams first. A number of analyzers including time-of-flight,[4] Wien filter,[5] retarding potential,[6] and magnetic mass spectrometers[7,8] have been used so far for mass measurements of cluster ions. However, these mass spectrometers are not ap-